Available online at www.sciencedirect.com

ScienceDirect

Ceramics International 40 (2014) 799–803

CERAMICS INTERNATIONAL

www.elsevier.com/locate/ceramint

Oxygen permeability of asymmetric membrane of functional $La_{0.8}Sr_{0.2}Cr_{0.5}Fe_{0.5}O_{3-\delta}$(LSCrF)–$Zr_{0.8}Y_{0.2}O_{2-\delta}$(YSZ) supported on porous YSZ

Wei Fang, Yu Zhang, Jianfeng Gao*, Chusheng Chen

CAS Key Laboratory of Materials for Energy Conversion, Department of Materials Science and Engineering, University of Science and Technology of China, Hefei Anhui 230026, China

Received 11 May 2013; received in revised form 16 June 2013; accepted 17 June 2013
Available online 6 July 2013

Abstract

An asymmetric membrane consisted of a thin functional layer and a thick support was developed for oxygen production and membrane reactors. The functional $La_{0.8}Sr_{0.2}Cr_{0.5}Fe_{0.5}O_{3-\delta}$(LSCrF)–$Zr_{0.8}Y_{0.2}O_{2-\delta}$(YSZ) layer was prepared by screen printing and the YSZ support by phase inversion tape casting. Performance of the membrane was evaluated under air/argon, air/CO and CO_2/H_2 gradient at 750–900 °C. The results indicate the membrane to have good chemical stability and considerable high oxygen permeability under stringent conditions. An oxygen permeation flux of 0.058, 0.175 and 1.198 ml (STP) cm^{-2} min^{-1} was obtained at 900 °C for operation under air/argon, CO_2/H_2 and air/CO gradient, respectively. The apparent activation energy for oxygen permeation was 131.22 ± 19.74, 89.53 ± 6.29 and 66.28 ± 1.41 kJ/mol under air/argon, air/CO and CO_2/H_2 gradient respectively. The results suggest the membrane to have potential applications in the chemical reactor.

Keywords: Oxygen separation membrane; Asymmetric; Membrane chemical reactor

1. Introduction

Oxygen separation membranes have attracted great attention due to their potential applications in the chemical reactor [1]. There are two main types of oxygen separation membranes currently. One type is single-phase membranes of mixed oxygen-ion and electron conductors. Among them, perovskites, such as (Ln, A)(Co, B)$O_{3-\delta}$ (Ln = rare earth elements, A = Ca, Sr, Ba, B = transition metal elements), have been extensively studied for applications, e.g. oxygen separation from air [2], syngas production by partial oxidation of methane [3], and hydrogen production from water splitting [4]. Although single-phase membranes show generally high oxygen permeability, their stability remains usually problematic, e.g. unstable under a reducing atmosphere for Co-containing single-phase membranes and very sensitive to CO_2 or CO for Ba-containing ones [5,6]. Another type is the so-called dual-phase composite membranes consisting of an oxide ionic conductor and an electronic conductor respectively [7]. With this composite strategy, materials selection may be flexible and it is easier to meet the requirements for a membrane operating under stringent conditions, nevertheless the oxygen permeability might be somewhat lower in comparison with a single-phase one [8]. Therefore, our group has recently focused on the research and development of dual-phase membranes, such as $La_{0.8}Sr_{0.2}Cr_{0.5}Fe_{0.5}O_{3-\delta}$(LSCrF)–$Zr_{0.84}Y_{0.16}O_{2-\delta}$(YSZ) composite [9].

Besides the materials, another important factor which affects greatly the oxygen permeation is the thickness of a membrane according to the Wagner equation [10]. Therefore, an asymmetric membrane, a thin functional dense layer supported on a porous substrate, is prevailing [11]. Over the years, various asymmetric membranes have been reported. Middleton et al. reported an asymmetric membrane of a thin dense layer of (La,Sr)(Co,Fe)O_3 supported on a porous MgO substrate [12]. Unfortunately the membrane cracks frequently due to thermal incompatibility of MgO and (La,Sr)(Co,Fe)O_3. Kovalevsky et al.

*Corresponding author. Tel.: +86 551 63601700.
E-mail address: jfgao@ustc.edu.cn (J. Gao).

0272-8842/$ - see front matter © 2013 Elsevier Ltd and Techna Group S.r.l. All rights reserved.
http://dx.doi.org/10.1016/j.ceramint.2013.06.070

reported a multilayer asymmetric membrane of $Ba_{0.5}Sr_{0.5}Co_{0.8}Fe_{0.2}O_{3-\delta}$ [13], using the same material for the functional layer and the porous support. The membrane shows high oxygen permeability under air/He gradient, but it is unstable under the atmospheres containing CO_2 and/or H_2O at elevated temperatures.

In order to solve the chemical stability problem fundamentally, the support of an asymmetric membrane could function only as a mechanical substrate. In addition, it should have an adequate porosity, a low resistance for gas transportation, and an appropriate thermal expansion coefficient matching with the functional layer. Y_2O_3-stabilized ZrO_2 (YSZ) is the most used electrolyte for high-temperature solid oxide fuel cells (SOFC). It has a high mechanical strength (300 MPa, 25 °C) and an appropriate thermal expansion coefficient ($\sim 10.8 \times 10^{-6}$), and has excellent stability under reductive and oxidative conditions at evaluated temperatures [14].

In this paper, we report an asymmetric membrane consisted of a thin functional layer of $La_{0.8}Sr_{0.2}Cr_{0.5}Fe_{0.5}O_{3-\delta}$(LSCrF)–$Zr_{0.8}Y_{0.2}O_{2-\delta}$(YSZ) and a thick support of YSZ. The membrane was prepared by phase inversion tape casting, screen printing and co-sintering. Performance of the membrane was examined under air/argon, air/CO and CO_2/H_2 gradient at 750–900 °C.

2. Experimental

A porous YSZ support of asymmetric membrane was first prepared by phase inversion tape casting [15]. The slurry was prepared by ball-milling, using commercial YSZ powders (d_{50}=0.8 μm, Fanmeiya, Anhui, China), N-methyl-2-pyrrolidone (NMP, CP, Sinopharm Chemical Reagent Co.) as solvent, polyethersulfone (PESf, Radel A-100, Solvay Advanced Polymers) as binder, and polyvinylpyrrolidone (PVP, K30, Sinopharm Chemical Reagent Co.) as dispersant. Dried green plate was then cut into discs with a diameter of 20 mm and pre-calcined at 900 °C for 2 h. The resulted YSZ support consisted of three layers, a thin skin layer with fine finger-like pores, a thick layer with finger-like voids and a thin sponge layer with fine pores. The sponge layer was polished off in order to improve gas transportation through the support. Subsequently, a functional layer of LSCrF–YSZ was prepared on the porous support (the skin layer side) by screen-printing and co-sintering at 1400 °C for 5 h. The slurry of LSCrF and YSZ with a volume ratio of 4:6 was prepared by ball-milling. LSCrF was synthesized via a conventional solid state reaction route [16]. For comparison, LSCrF–YSZ disk-shaped symmetric membrane was prepared by a uniaxial pressing method [9].

The oxygen permeation of the as-prepared membrane was measured under air/argon, air/CO and CO_2/H_2 gradient at 750–900 °C, using a home-made setup with an online gas chromatography (GC9790II, Fuli, China) equipped with a thermal conductivity detector and two columns, one filled with 5A molecular sieves for oxygen and nitrogen detection and the other with TDX-01 for H_2, CO and CO_2 detection (Fig. 1). For all the tested samples, the dense layer side was exposed to air (or CO_2) with a flowing rate of 30 ml min^{-1} and the porous support side was swept with argon (or CO or H_2) with a flowing rate of 30 ml min^{-1}. X-ray diffraction analysis (XRD, X'Pert Pro, Phillips, Netherlands) was used to examine the

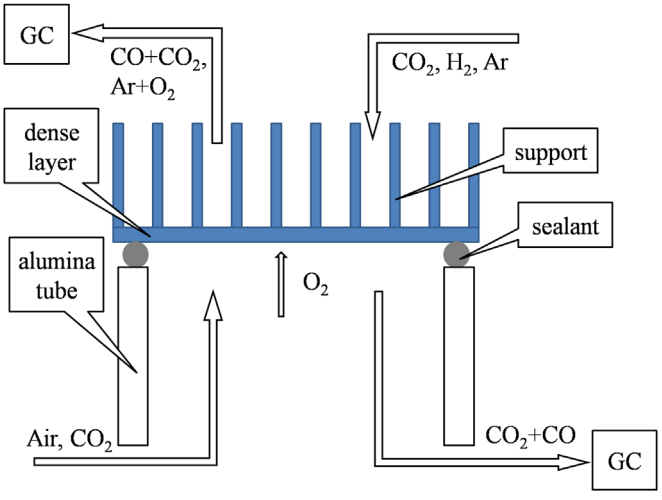

Fig. 1. Schematic diagram of the experimental setup for oxygen permeation measurement.

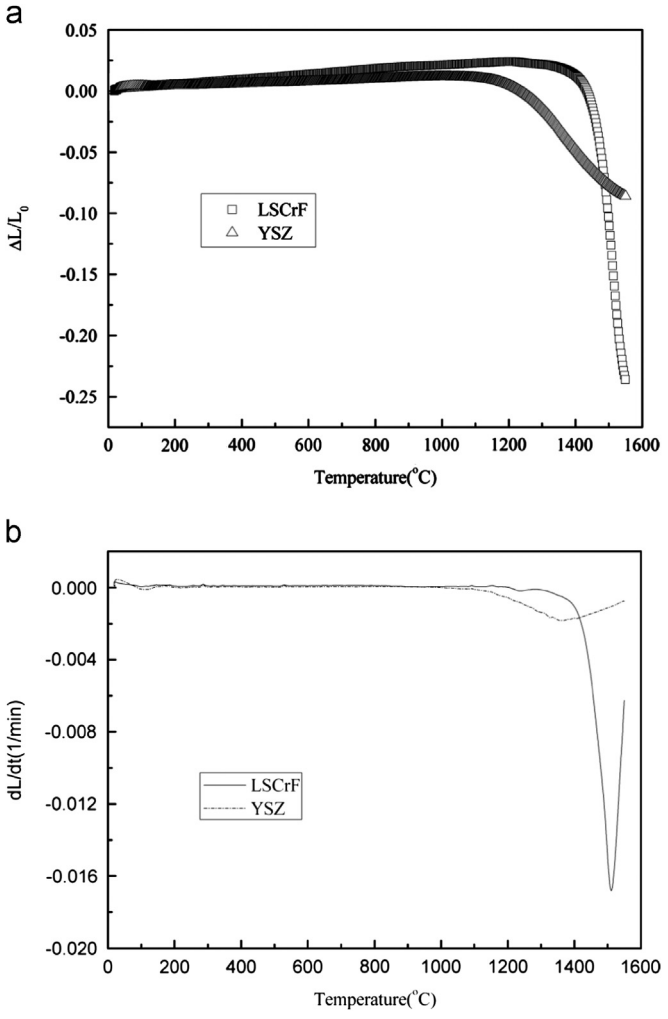

Fig. 2. Dilatometric curves of LSCrF and YSZ (a) sintering curves and (b) sintering rate curves.

structure of pre- and post-tested samples. Morphology of micro structure was observed on scanning electron microscopy (SEM, JSM-6390LA, JEOL, Japan).

3. Results and discussion

In order to deliver a clearer picture of sintering behaviors of dual-phase membrane materials, shrinkage of LSCrF and YSZ was investigated first and is shown in Fig. 2. As it can be seen in Fig. 2(a), the temperature for final shrinkages of these ceramics at around 1400 °C decreases in the order of YSZ, and LSCrF; while the temperature for initial shrinkages increases in the order of YSZ, and LSCrF. Moreover, the temperature for the highest sintering rates of these ceramics increases in the order of YSZ (1327 °C) and LSCrF (1511 °C), while the highest sintering rate decreases in the order of LSCrF, and YSZ (Fig. 2(b)).

Fig. 3 shows XRD patterns of the pre- and post-tested membranes. It shows that the functional layer consisted of cubic YSZ and perovskite-type LSCrF as main phases. It implies that the materials are stable in the preparation process and under the operation conditions. Unlike the YSZ–$La_{0.8}Sr_{0.2}MnO_3$ composite, no $La_2Zr_2O_7$ phase was significantly found in this composite, and the composite was stable under stringent conditions for the 500 h oxygen permeation test in our previous work [16].

Fig. 4 shows SEM views of the post-tested membrane. The porous YSZ support has a dual-pore structure, the large finger-like pore layer with a thickness of about 450 μm and the fine finger-like pore layer with a thickness of about 60 μm (Fig. 4a). With this structure, some advantages can be expected: the thick large pore layer offers a high mechanical strength for the functional layer and a low resistance for gas transportation, while the thin fine pore layer neighboring with the dense functional layer improves the active sites for the surface reactions. The dense functional layer with a thickness of about 120 μm is well adhered on the support. The functional layer has a gastight bulk (Fig. 4b) but a porous surface (Fig. 4c). And the porous surface is also beneficial for the relative surface exchange kinetics. For the post-tested membrane (testing time more than 150 h), no significant change is observed, and the result is consistent with the previous work [9,16].

The oxygen permeability is always important for a membrane targeting practical applications. For every tested sample in our experiments, gas tightness was first checked under air/argon gradient at 900 °C. Only for those that the leakage was less than 1%, oxygen permeation measurements were then carried out under air/argon, air/CO and CO_2/H_2 gradient respectively. Leakage due to imperfect sealing was subtracted when calculating the oxygen permeation fluxes. Fig. 5 is the

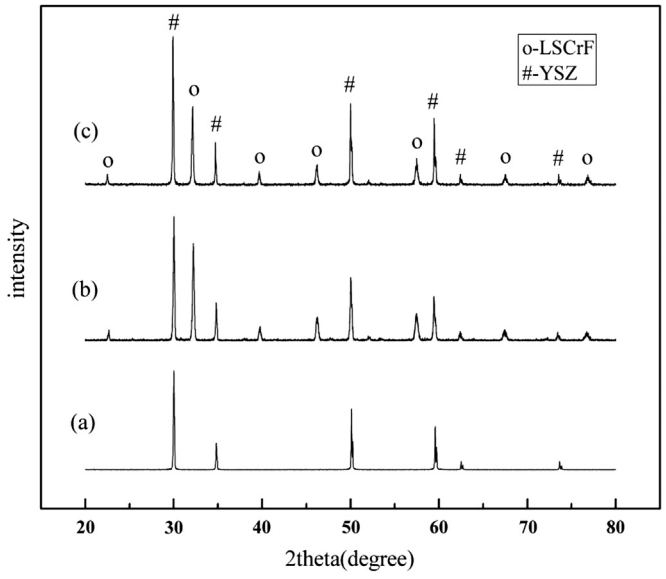

Fig. 3. XRD patterns of the post-tested support (a), the pre-tested (b) and post-tested (c) functional layer, (○) LSCrF, (#) YSZ.

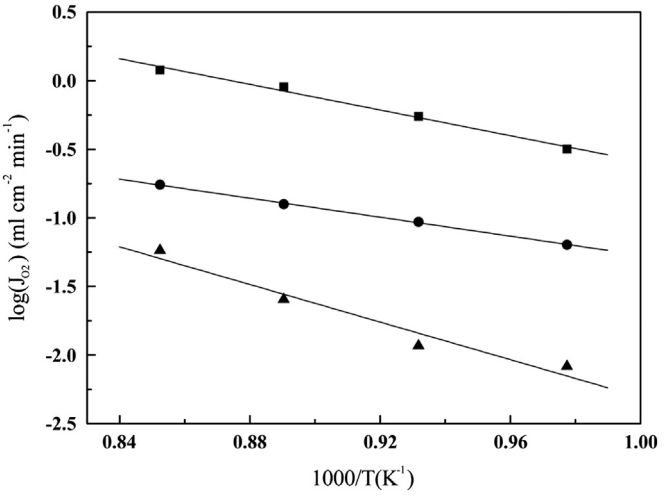

Fig. 5. Arrhenius plots of oxygen permeation fluxes of the asymmetric membrane under (●) CO_2/H_2, (■) air/CO and (▲) air/argon gradient.

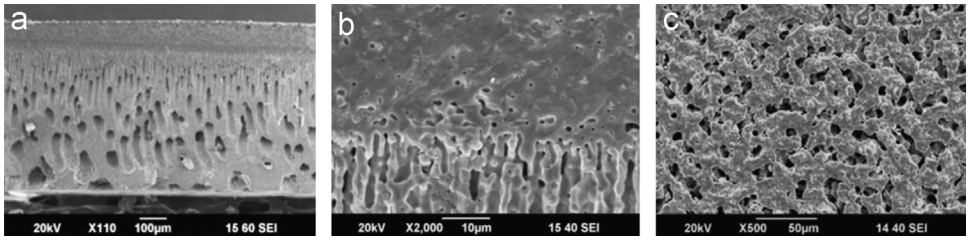

Fig. 4. SEM images of the post-tested asymmetric membrane, the cross-section view (a), the interface of functional layer and porous support (b), and the surface of the functional LSCrF–YSZ layer (c).

Arrhenius plots of oxygen permeation. The as-prepared asymmetric membrane exhibits acceptable oxygen permeability, increasing with operation temperature over the testing temperature range. At 900 °C, the oxygen permeation flux reached about 0.058, 0.175 and 1.198 ml (STP) cm^{-2} min^{-1} under air/argon, CO_2/H_2 and air/CO gradient respectively. At first glance, the oxygen fluxes agree with the Wagner equation [10], a higher oxygen partial pressure difference ($p^h_{O_2}/p^l_{O_2}$) across a membrane results in a larger oxygen flux, and the difference is about 10^3, 10^{16} and 10^{19} for air/argon, CO_2/H_2 and air/CO gradient respectively. But in fact the data does not follow strictly the order as calculated by the Wagner equation. The oxygen flux should be somewhat higher than the appeared value for the membrane under CO_2/H_2 gradient if the oxygen permeation follows strictly the Wagner theory for the membrane under all the different operation conditions. Therefore, the permeation is not simply controlled by the bulk diffusion, but also affected by the surface reactions. The calculated activation energy for oxygen permeation was 131.22 ± 19.74, 89.53 ± 6.29 and 66.28 ± 1.41 kJ/mol for the membrane under air/argon, air/CO and CO_2/H_2 gradient respectively. The apparent activation energy is much lower for the membrane under air/CO or CO_2/H_2 than that under air/argon gradient. It may be explained as that CO or H_2 has a higher activity and results in enhanced surface reaction kinetics, or it can be attributed to that the atmospheres of air/CO or CO_2/H_2 has led to an increase in the surface oxygen exchange kinetics and a change in the chemical defects of the membrane and the surface (including a changed ambipolar conductivity of the membrane) [17]. But the detail is needed for further study in the near future.

Fig. 6 shows the oxygen permeation fluxes of the asymmetric membrane and the symmetric membrane under CO_2/H_2 gradient. A much higher oxygen permeation flux of 0.175 ml (STP) cm^{-2} min^{-1} was observed at 900 °C with the asymmetric membrane, while only 0.026 ml (STP) cm^{-2} min^{-1} for the LSCF–YSZ disk-shaped symmetric membrane. And the functional layer thickness of the asymmetric membrane is ~120 μm, while ~1 mm for the symmetric membrane. The result indicates that the oxygen permeation flux can be increased significantly by reducing the thickness of the membrane [17].

Fig. 7 shows the dependence of oxygen permeation flux on the sweeping rate of H_2 for the membrane under CO_2/H_2 gradient. The oxygen permeation flux increases significantly with the sweeping rate from 4.5 to 22 ml/min, but it shows little response to a further increase in the sweeping rate. At the first stage, an increase in the sweeping rate leads to a decrease in the oxygen partial pressure of the gas phase and the thickness of the surface boundary layer, so it improves the surface exchange and favors the diffusion of relative active masses from the gas phase to the surface, while at the last stage a further increase in the sweeping rate would have a lesser or little effect on those.

In this primary research, electrolyte YSZ with negligible electronic conductivity was used for the porous support. Herewith the relative surface reactions would be restricted almost in the interface between the functional layer and the support. It is not in favor of the surface exchange kinetics. Therefore, it should be optimized by incorporating some electronic materials into the porous YSZ support in the future work, to extend the reaction region into the support, increase the three-phase boundary and surface reaction active sites, and improve the surface exchange kinetics.

4. Conclusions

The asymmetric membrane consisted of a functional $La_{0.8}Sr_{0.2}Cr_{0.5}Fe_{0.5}O_{3-\delta}$(LSCrF)–$Zr_{0.8}Y_{0.2}O_{2-\delta}$(YSZ) layer and a porous YSZ support was successfully prepared by phase inversion tape casting, screen printing and co-sintering. It shows acceptable oxygen permeability and good stability under air/CO and CO_2/H_2 gradient. The results suggest potential applications in the recycling of CO_2 and chemical reactors. However, optimization of the membrane and more understanding

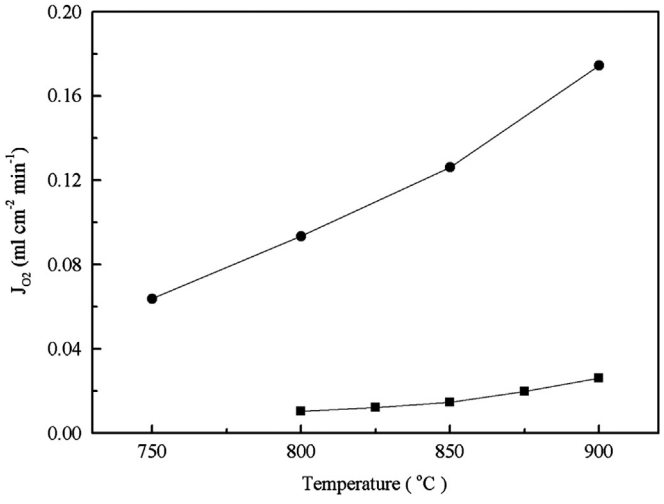

Fig. 6. Oxygen permeation fluxes of (●) the asymmetric membrane and (■) the symmetric membrane under CO_2/H_2 gradient.

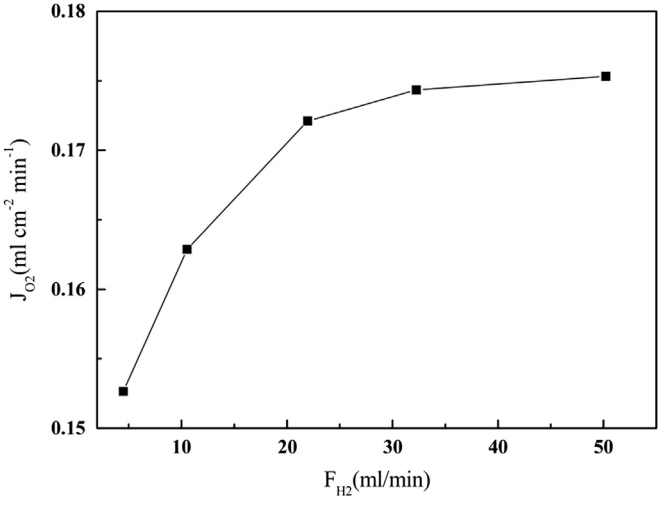

Fig. 7. The dependence of oxygen permeation fluxes of the asymmetric membrane on the sweeping rate of H_2 under CO_2/H_2 gradient at 900 °C.

on the membrane process, particularly about the relative surface reaction kinetics, is needed in the near future.

Acknowledgment

This work is supported by the National Natural Science Foundation of China (Grant nos. 21176230 and 21041010).

References

[1] K. Li, Ceramic Membranes for Separation and Reaction, Wiley, Chichester, England, 2007.
[2] Z.H. Chen, R. Ran, Z.P. Shao, H. Yu, J.C. Costa, S.M. Liu, Further performance improvement of $Ba_{0.5}Sr_{0.5}Co_{0.8}Fe_{0.2}O_{3-\delta}$ perovskite membranes for air separation, Ceramics International 35 (2009) 2455–2461.
[3] U. Balachandran, J.T. Dusek, R.L. Mieville, R.B. Poeppel, M.S. Kleefisch, S. Pei, et al., Dense ceramic membranes for partial oxidation of methane to syngas, Applied Catalysis A 133 (1995) 19–29.
[4] H.Q. Jiang, H.H. Wang, S. Werth, T. Schiestel, J. Caro, Simultaneous production of hydrogen and synthesis gas by combining water splitting with partial oxidation of methane in a hollow-fiber membrane reactor, Angewandte Chemie International Edition 47 (2008) 9341–9344.
[5] M. Arnold, H.H. Wang, A. Feldhoff, Influence of CO_2 on the oxygen permeation performance and the microstructure of perovskite-type $(Ba_{0.5}Sr_{0.5})(Co_{0.8}Fe_{0.2})O_{3-\delta}$ membranes, Journal of Membrane Science 293 (2007) 44–52.
[6] J.X. Yi, S.M. Feng, Y.B. Zuo, W. Liu, C.S. Chen, Oxygen permeability and stability of $Sr_{0.95}Co_{0.8}Fe_{0.2}O_{3-\delta}$ in a CO_2- and H_2O-containing atmosphere, Chemistry of Materials 17 (2005) 5856–5861.
[7] V.V. Kharton, A.V. Kovalevsky, A.P. Viskup, A.L. Shaula, F.M. Figueiredo, E.N. Naumovich, et al., Oxygen transport in $Ce_{0.8}Gd_{0.2}O_{2-\delta}$-based composite membranes, Solid State Ionics 160 (2003) 247–258.
[8] W. Li, J.J. Liu, C.S. Chen, Hollow fiber membrane of yttrium-stabilized zirconia and strontium-doped lanthanum manganite dual-phase composite for oxygen separation, Journal of Membrane Science 340 (2009) 266–271.
[9] Y.L. Luo, T. Liu, J.F. Gao, C.S. Chen, $Zr_{0.84}Y_{0.16}O_{1.92}$–$La_{0.8}Sr_{0.2}Cr_{0.5}Fe_{0.5}O_{3-\delta}$ composite membrane for CO_2 decomposition, Materials Letters 86 (2012) 5–8.
[10] S.J. Xu, W.J. Thomson, Oxygen permeation rates through ion-conducting perovskite membranes, Chemical Engineering Science 54 (1999) 3839–3850.
[11] W.Q. Jin, S.G. Li, P. Huang, N.P. Xu, J. Shi, Preparation of an asymmetric perovskite-type membrane and its oxygen permeability, Journal of Membrane Science 185 (2001) 237–243.
[12] H. Middleton, S. Diethlm, R. Ihringer, D. Larrain, J. Sfeir, J.V. Herle, Co-casting and co-sintering of porous MgO support plates with thin dense perovskite layers of $LaSrFeCoO_3$, Journal of the European Ceramic Society 24 (2004) 1803–1806.
[13] A.V. Kovalevsky, A.A. Yaremchenko, V.A. Kolotygin, F.M.M. Snijkers, V.V. Kharton, A. Buekenhoudt, et al., Oxygen permeability and stability of asymmetric multilayer $Ba_{0.5}Sr_{0.5}Co_{0.8}Fe_{0.2}O_{3-\delta}$ ceramic membranes, Journal of Membrane Science 192 (2011) 677–681.
[14] N.Q. Minh, T. Takahashi, Science and Technology of Ceramic Fuel Cells, Elsevier, Amsterdam, The Netherlands 75–80.
[15] C. Jin, C.H. Yang, F.L. Chen, Effects on microstructure of NiO–YSZ anode support fabricated by phase-inversion method, Journal of Membrane Science 363 (2010) 250–255.
[16] J.J. Liu, T. Liu, W.D. Wang, J.F. Gao, C.S. Chen, $Zr_{0.84}Y_{0.16}O_{1.92}$–$La_{0.8}Sr_{0.2}Cr_{0.5}Fe_{0.5}O_{3-\delta}$ dual-phase composite hollow fiber membrane targeting chemical reactor applications, Journal of Membrane Science 389 (2012) 435–440.
[17] H.J.M. Bouwmeester, A.J. Burggraaf, Dense ceramic membranes for oxygen separation, in: A.J. Burggraaf, L. Cot (Eds.), Fundamentals of Inorganic Membrane Science and Technology, Elsevier, Amsterdam, 1996, pp. 435–528.